ENSO Influence on Intraseasonal Extreme Rainfall and Temperature Frequencies in the Contiguous United States: Observations and Model Results

ALEXANDER GERSHUNOV AND TIM P. BARNETT

Climate Research Division, Scripps Institution of Oceanography, University of California, San Diego, La Jolla, California

(Manuscript received 27 January 1997, in final form 29 August 1997)

ABSTRACT

The signature of ENSO in the wintertime frequencies of heavy precipitation and temperature extremes is derived from both observations and atmospheric general circulation model output for the contiguous United States. ENSO signals in the frequency of occurrence of heavy rainfall are found in the Southeast, Gulf Coast, central Rockies, and the general area of the Mississippi–Ohio River valleys. Strong, nonlinear signals in extreme warm temperature frequencies are found in the southern and eastern United States. Extreme cold temperature frequencies are found to be less sensitive to ENSO forcing than extreme warm temperature frequencies. Observed ENSO signals in extreme temperature frequencies are not simply manifestations of shifts in mean seasonal temperature. These signals in the wintertime frequency of extreme rainfall and temperature events appear strong enough to be useful in long-range regional statistical prediction.

Comparisons of observational and model results show that the model climate is sensitive to ENSO on continental scales and provide some encouragement to modeling studies of intraseasonal sensitivity to low-frequency climatic forcing. However, large regional disagreements exist in all variables. Continental-scale El Niño signatures in intraseasonal temperature variability are not correctly modeled. Modeled signals in extreme temperature event frequencies are much more directly related to shifts in seasonal mean temperature than they are in nature.

1. Introduction

Long-range predictability of extreme event frequencies depends on the sensitivity of the intraseasonal probability density functions' (PDFs') tails to known and predictable interannual climatic signals. An intraseasonal PDF could, for example, be the PDF of daily temperature for a winter season at a particular location. The El Niño–Southern Oscillation (ENSO) is the largest known and predictable climatic signal at the seasonal to interannual timescale. The ENSO-related evolution of tropical Pacific sea surface temperature (SST) anomalies is predictable with coupled models out to lead times of 18 months with highest skill in the central equatorial Pacific for the boreal winter (e.g., Cane and Zebiak 1985; Barnett et al. 1993). Central equatorial Pacific SST anomalies are well known to influence extratropical climate, specifically, midlatitude Northern Hemispheric circulation patterns during boreal winter (e.g., Wallace and Gutzler 1981). ENSO signatures in seasonal mean surface climate partially described by several researchers (see references below) suggest that intraseasonal variability in the midlatitudes should also experience interannual modulation associated with ENSO. The main purpose of this work is to provide a broad assessment of ENSO's influence on the U.S. wintertime frequency of extreme events. In this regard, we focus on the tails of intraseasonal precipitation and temperature PDFs. A qualitative assessment of predictability is achieved through the evaluation and comparison of natural and modeled ENSO-related anomaly patterns of extreme daily precipitation and temperature event frequencies.

The heavy one-tailed nature of daily precipitation distributions for most seasons and locations around the world is such that a very small number of heavy precipitation events account for a disproportionately large share of the monthly, seasonal, and longer-term total precipitation. For example, it is typical for most seasons and stations that over 50% of the rainfall falls in fewer than 20% of the rain days. Besides this important contribution to the freshwater supply, heavy precipitation events directly affect human welfare through their close association with hydrological disasters such as floods, mudslides, etc. Long-range prediction of the frequency of heavy precipitation would therefore be an extremely useful capability. In contrast to the rainfall PDFs, the intraseasonal temperature distribution is two tailed so that extreme events occur in both the cold and warm tails of the distribution. Seasonal frequencies of extreme cold and heat also strongly influence human, agricultural, and economic welfare of society (e.g., Pan et al. 1995; Brown et al. 1986; Changnon and Vonnahme

Corresponding author address: Dr. Alexander Gershunov, Climate Research Division, Scripps Institution of Oceanography, University of California, San Diego, 9500 Gilman Dr., La Jolla, CA 92093-0224.

1986) so that their skillful prediction would, likewise, be of enormous value.

So far, the ENSO signal in the U.S. seasonal and monthly precipitation totals and average temperatures has been partially described for some regions by Kiladis and Diaz (1989), Ropelewski and Halpert (1986, 1996), and Redmond and Cayan (1994). The effect of ENSO phases on daily rainfall frequency and intensity was also examined for the western United States by Cayan and Webb (1992), Woolhiser et al. (1993), and Cayan et al. (1996). All these studies point to the fact that large regions of the United States experience significant modulation of winter rainfall and temperature by ENSO. The daily rainfall studies for the western United States suggest that rain tends to be stronger and more frequent in the southwest during El Niño winters compared to La Niña winters. The opposite signal is observed for the Northwest. Particularly interesting is the evidence presented by Cayan et al. (1996) suggesting that the ENSO signal in daily rainfall frequencies is accentuated for heavy rainfall events in the western United States. Given these results, and the dependence of monthly to seasonal average rain amounts on the frequency of extreme rain events, it is reasonable to expect to find a modulation of the frequency of daily rainfall extremes by ENSO, at least for preferred locations in winter. Although daily temperature extremes exert less influence on seasonal means than is the case with precipitation, ENSO-related shifts in seasonal means are manifestations of ENSO modulation of the seasonal distributions of daily temperatures. Does ENSO simply shift the whole seasonal distribution of daily temperature, does it change its basic shape, or both? In other words, does it affect the mean, the higher moments, or both? Do shifts in the central tendency translate into changing probabilities of extreme events? Can expected frequencies of extreme events change without shifts in the mean? What are the geographical patterns of these sensitivities? These questions cannot be answered by considering seasonal or monthly mean temperatures or total precipitation. Our primary concern is with ENSO sensitivity of the distributions' tails. We therefore undertake to describe the empirical patterns of this sensitivity for the winter season in the contiguous United States.

Corresponding patterns generated by an atmospheric GCM forced by observed global SST are also derived. Regional verifications of GCM intraseasonal statistics are rarely carried out, even for climatology or the seasonal cycle. GCM climatology of high-frequency precipitation statistics for January and July and regional seasonal cycles have only recently been compared with observations for the contiguous United States (Chen et al. 1996). Sensitivity of GCMs to low-frequency climatic forcing has been examined only on monthly and longer timescales (e.g., Lau 1985; Graham et al. 1994; Graham and Barnett 1995). However, despite the lack of evidence that modeled intraseasonal statistics respond correctly to low-frequency climatic variability, GCMs

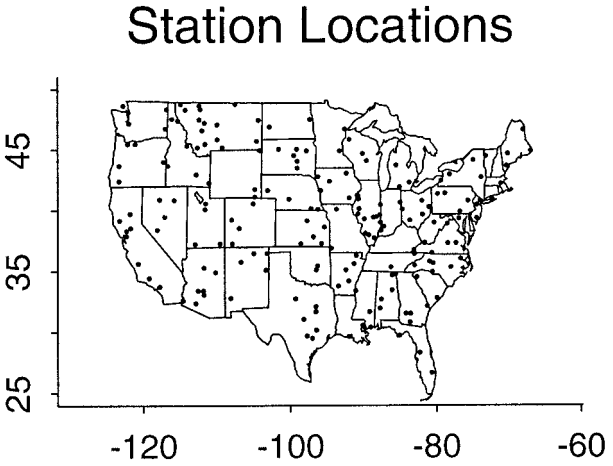

FIG. 1. Dots represent station locations for the 184 stations used in this study.

are commonly used to make global and regional ''predictions'' of intraseasonal variability under enhanced CO_2 climate (e.g., Intergovernmental Panel on Climate Change 1990, hereafter IPCC; Cubasch et al. 1995; Gregory and Mitchell 1995; Barrow and Hulme 1996). Hence, one purpose of such a comparison is to shed light on the utility of modern GCMs in predicting changes in intraseasonal climatic variability associated with low-frequency climatic forcing. A more direct aim of this exercise is to point out areas of agreement and disagreement between natural and modeled response to ENSO and to qualitatively assess the predictive potential of U.S. intraseasonal variability in a state of the art GCM with regard to ENSO teleconnections.

Data and methodology are described in sections 2 and 3, respectively. Section 4 presents and compares results for precipitation and temperature for nature and a model. A summary with conclusions are found in section 5.

2. Data

Observational data are daily rainfall totals and average temperatures (averages of daily maximum and minimum temperature) from the National Climatic Data Center (NCDC) (courtesy of T. Karl) recorded at 184 stations scattered more or less uniformly across the contiguous United States spanning the period from the early 1900s to 1993. We shall concentrate on the period 1950–93 for reasons that will become obvious. Station locations are denoted by dots in Fig. 1.

The atmospheric GCM used to simulate contemporaneous daily weather is the ECHAM3 model developed at the Max-Plank Institute at the University of Hamburg. ECHAM3 is the most successful of 29 atmospheric GCMs ranked according to their ability to simulate various aspects of the observed hydrologic cycle on various space timescales (Lau et al. 1996). The model was forced with observed global SST over the period 1950–

94 and so, model-generated interannual variability contains the ENSO signal by design. The spatial resolution is T42 (roughly 2.8° × 2.8°).

The model tends to produce a relatively persistent drizzle in some areas, so, in order to match model rainfall frequency with that observed in nature, all model daily totals smaller than 1 mm are set to zero. Although GCMs tend to systematically underestimate the frequency of light precipitation over tropical and subtropical regions characterized by persistent low-level stratocumuli (Lau et al. 1996), overestimation of rainfall frequency may be a common GCM feature over midlatitude continents. This problem was also noticed by Chen et al. (1996) in the National Center for Atmospheric Research Community Climate Model version 2/Biosphere–Atmosphere Transfer Scheme. Incidentally, as a welcome side effect, removal of model drizzle produces a more realistic shape of the rainfall PDFs reflected in realistic daily rainfall rate quantiles (see below).

3. Methods

a. ENSO compositing

A compositing approach based on contemporaneous central tropical Pacific SST (PAC3: SST averaged over 170°–120°W, 5°S–5°N) is used to isolate the ENSO signal during December, January, and February (DJF). This measure is used for several reasons. A connection between tropical central Pacific SST and the extratropical large-scale circulation has been well established over the last two decades. Also, coupled models of the tropical Pacific exhibit good predictive skill in this region up to 18 months before the onset of anomalous SST (Barnett et al. 1993). These models are especially skillful in predicting boreal winter SST anomalies. El Niño (La Niña) years are defined here as those years in which PAC3 was more than one standard deviation above (below) the mean. We refer to El Niño years as ''warm'' years, La Niña years as ''cold'' years, and all other years as ''base'' years. Warm years' Januaries fall into 1958, 1964, 1966, 1969, 1970, 1973, 1983, 1987, and 1992, while cold years' Januaries fall into 1951, 1956, 1971, 1974, 1976, 1985, and 1989.

This compositing approach allows meaningful comparisons between modeled and observed climatic signals. The stochastic nature of the GCM climate forecasting problem is well known (e.g., Barnett 1995; Lau et al. 1996). A single model run cannot constitute a meaningful forecast of a particular event. Rather, multiple model realizations are required. The compositing approach adopted here in effect provides a multiple model realization forecast for the canonical ENSO event. In other words, a single long model run is used to provide a GCM forecast signature of the canonical ENSO event in the same sense as multiple model realizations can be used to provide a forecast signature of a single event.

b. Frequencies of extremes

To isolate heavy precipitation events, we focus on the right (and only) tail of the daily DJF rainfall distribution by computing the 75th percentile from the base years' daily rainfall totals considering only days with measurable precipitation ($\geq$0.25 mm day^{-1} for station data and $\geq$1 mm day^{-1} for ECHAM3). Percentile maps for the United States are shown in the upper panels of Fig. 2. We then compute the percentage of warm and cold years' DJF rain days with daily amounts greater than the base years' 75th percentile. This percentage value (P) is adjusted for the fact that frequency of rain days (f) is also modulated by ENSO. The adjustment is made by multiplying the percentage value by the frequency of rain days in anomalous winters relative to that in base years. For example, say that at some location (station or grid cell) during cold event winters, the percentage of daily rain events with daily totals exceeding the 75th base percentile is 20% ($P_c = 20$). Furthermore, say that the frequency of rainy days (defined as the proportion of days with precipitation) during base years is 0.3 ($f_b = 0.3$) while during cold years, $f_c = 0.2$. Frequency-adjusted percentage for that location for cold years is expressed as follows: $P_{\text{adj}} = (f_c/f_b)P_c = 13.3\%$. Adjusted percentage is expressed as an anomaly in percent of expected number of events ($P_{\text{anom}} = 100(P_{\text{adj}}/P_b - 1)$, where P_b is the percentage value in base years or, by definition, the relative weight of the PDF's tail: 100 − the percentile). For the above example, $P_{\text{anom}} = 100(13.3/25 - 1) = -46.7$, that is, a 46.7% decrease in the frequency of heavy precipitation events during cold event winters relative to base winters. Maps of adjusted percentage anomalies of heavy winter rainfall events are displayed in Fig. 2. Warm and cold years' frequency anomaly maps are found in the middle and bottom plates, respectively. Observed results are delineated on the left side of the figures, while model-generated results are on the right.

A similar analysis is performed on the temperature data with the following exceptions. Since temperature is not an episodic variable, no frequency adjustment is necessary or possible. Since both hot and cold extremes are important, both tails of the temperature distributions are considered. Extreme hot (cold) events are defined as those days with temperatures above (below) the base years' 95th (5th) percentile. So, for example, if at some station during anomalous winters, the percentage of days with temperatures below the base winters' 5th percentile is 10%, then the cold extreme frequency anomaly is $P_{\text{anom}} = 100(10/5 - 1) = 100$, that is a 100% increase in the frequency of cold extremes during anomalous winters relative to base winters. Results for warm and cold extremes (right and left PDF tails) are displayed in Figs. 3 and 4, respectively, in the same format as

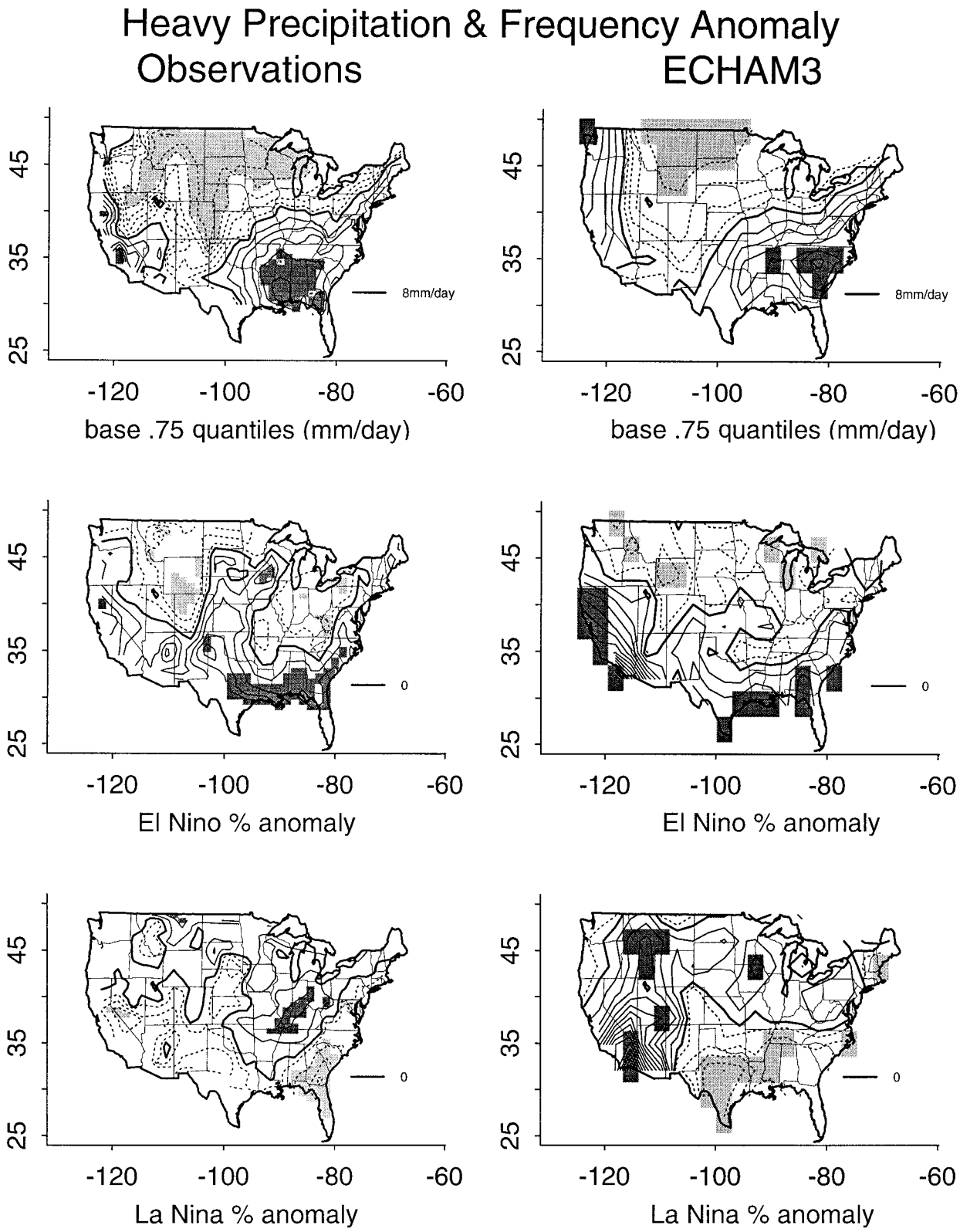

FIG. 2. (upper panels) The 75th percentile of base years' DJF daily precipitation distribution for days with precipitation. The 8-mm contour is thickened. Contours <8 mm are dashed at 1-mm intervals. Contours >8 mm are solid at 2-mm intervals. Values <4 mm day^{-1} (>16 mm day^{-1}) are lightly (darkly) shaded. (middle panels) Frequency-adjusted percentage anomaly (see text) of observations during warm years *wetter* than base years' 75th percentile. The zero contour is thickened. Negative (positive) contours are dashed (solid), delineated at 15%

those for precipitation extremes. For reasons to become clear below, above-median (50th percentile) temperature frequency anomalies are displayed in Fig. 5.

A note about interpreting the temperature results is in order here. The DJF part of the seasonal cycle in temperature and precipitation undergoes an evolution. Day-to-day variability can also differ from month-to-month. For DJF, these effects are much more consistent in both space and time for daily temperature than for precipitation. The most consistent of these effects is the fact that, climatologically, January tends to be the coldest month in most places in the Northern Hemisphere, although this is frequently not the case in individual winters. In the contiguous United States, the range of the observed and modeled seasonal cycles in DJF is typically less than 2°C. The intramonthly range of daily average temperatures typically exceeds the DJF seasonal range by more than an order of magnitude. Because variability due to the DJF portion of the seasonal cycle is small compared to the intraseasonal variability considered here, the seasonal cycle is not removed. In the following discussion, the reader should be aware that the extreme temperature results may be slightly biased in time: warm (cold) daily extreme frequencies will tend to emphasize the middle (ends) of the DJF time window. For longer definitions of the winter season (e.g., November–March), this could become a serious problem that would have to be dealt with by subtracting the mean seasonal cycle from the daily data and, perhaps, also scaling by the seasonally evolving standard deviation.

c. Significance testing

Statistical significance is assessed on all frequency anomaly maps in order to separate the ENSO signal from noise. This is done via the bootstrap resampling technique (Efron 1982). Winters representing warm and cold composites were randomly picked without replacement from the set of *all* 43 winters on record. Composites of 9 and 7 random winters were used to estimate the accidental frequency anomaly (noise) associated with the El Niño and La Niña composites, respectively, relative to the remaining 27 winters representing the random base composite. This procedure was repeated 100 times for each observed and modeled precipitation and temperature frequency variable as defined above. Local positive and negative frequency anomalies are considered significant at the 0.1 significance level if their absolute magnitudes exceed the 95th and 5th percentiles of the bootstrapped accidental anomaly (noise) distribution, respectively. Statistically significant frequency anomalies are delineated on all frequency anomaly maps by shading.

4. Discussion

a. Precipitation extremes

The spatial patterns of the 75th percentile for DJF daily rainfall during base years (Fig. 2, upper panels) are very similar for observations and model. These maps define what heavy precipitation means in various parts of the country. Low values are indicative of the generally slight precipitation throughout northern continental areas protruding southward into the west and lee of the Rockies. Here, daily precipitation totaling over 3–4 mm is considered heavy. The model overestimates the magnitude of the 75th percentile by $\sim$1 mm day^{-1} throughout the northern United States and by up to 8 mm day^{-1} in the northwest. High rainfall percentiles in the southeast (with a maximum centered on Mississippi and Alabama in the observations and Carolinas in the model) and along the West Coast suggest that in these parts of the country, heavy rainfall is defined as daily total precipitation exceeding 14–18 mm day^{-1}. Western slopes of the Rockies are marked with somewhat higher than surrounding observed percentiles, whereas coarse resolution precludes the model from resolving this feature. Likewise, the model cannot resolve the rainshadow effect of the Sierras and Cascades apparent in the observations. As mentioned earlier, the very good general agreement between the magnitudes of modeled and observed 75th precipitation percentile is a consequence of the removal of model drizzle.

The middle panels of Fig. 2 show the El Niño signal in the percent change of heavy rainfall frequency. These are the adjusted percentage anomaly maps (P_{anom}) where the value expected in the absence of any signal is 0%. However, spurious signal (noise) can be generated by chance. This is essentially what has been done with the bootstrap. In some regions characterized by large outliers, the noise can be rather large. As a result, seemingly large percentage anomalies may not be statistically different from zero. The following discussion focuses on statistically significant and spatially coherent patterns. Discussion of noisy results is limited to the largest-scale patterns. The term ''signal'' is reserved for statistically significant patterns. Highly localized signals are not discussed.

The El Niño signal in observations is as follows: central Rockies experience 30% fewer than expected heavy rainfall events, while the frequency of heavy rainfall events is enhanced by 15%–30% in the southeast, especially along the southeastern seaboard, the Gulf

←

intervals. Positive (negative) values found to be statistically significant at the 0.1 significance level are darkly (lightly) shaded. (lower panels) Same as middle panels but for cold years. (left panels) Observational results. (right panels) Model results.

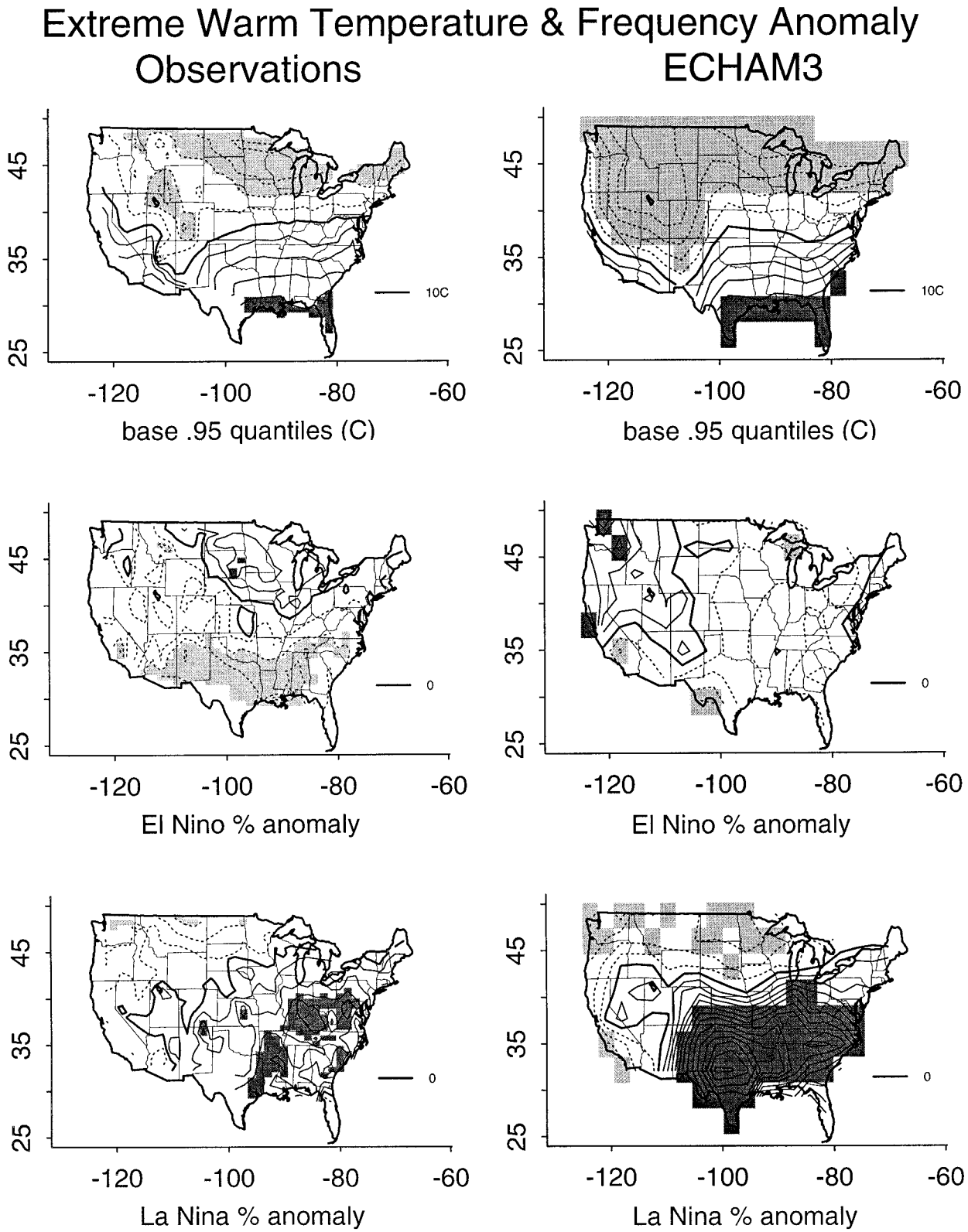

FIG. 3. (upper panels) The 95th percentile of base years' DJF daily average temperature distribution. The 10°C contour is thickened. Contours <10°C (>10°C) are dashed (solid) at 2.5°C intervals. Values <5°C (>20°C) are lightly (darkly) shaded. (middle panels) Percentage anomaly of observations during warm years *warmer* than base years' 95th percentile. The zero contour is thickened. Negative (positive) contours are dashed (solid), delineated at 20% intervals. Positive (negative) values found to be statistically significant at the 0.1 significance level are darkly (lightly) shaded. (lower panels) Same as middle panels but for cold years. (left panels) Observational results. (right panels) Model results.

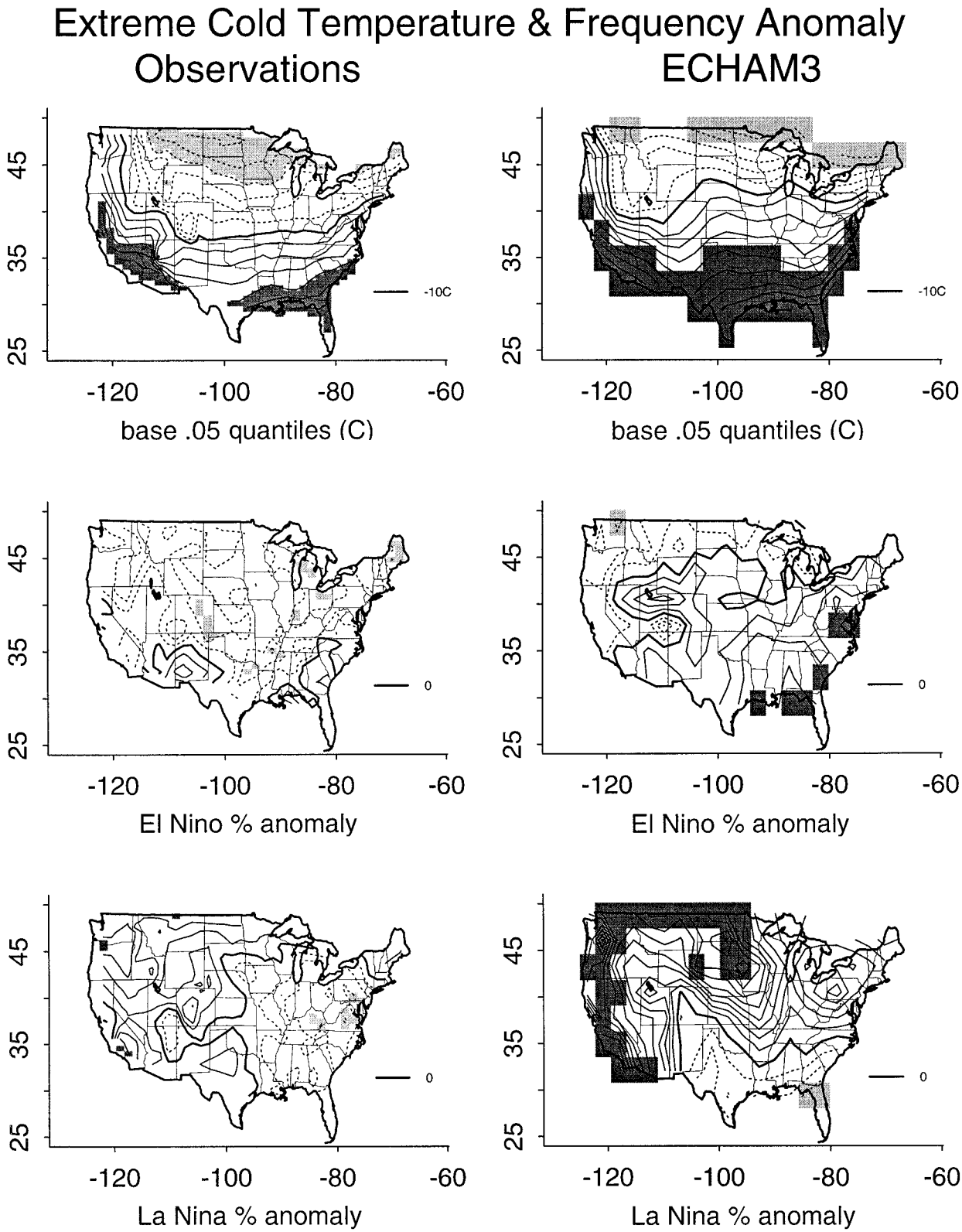

FIG. 4. (upper panels) The 5th percentile base years' DJF daily average temperature distribution. The −10°C contour is thickened. Contours <−10°C (>−10°C) are dashed (solid) at 2.5°C intervals. Values <−20°C (>0°C) are lightly (darkly) shaded. (middle panels) Percentage anomaly of observations during warm years *colder* than base years' 5th percentile. The zero contour is thickened. Negative (positive) contours are dashed (solid), delineated at 20% intervals. Positive (negative) values found to be statistically significant at the 0.1 significance level are darkly (lightly) shaded. (lower panels) Same as middle panels but for cold years. (left panels) Observational results. (right panels) Model results.

Coast, and the Texas panhandle. A small but coherent region of enhanced heavy precipitation frequency is located at the confluence of the Mississippi and Wisconsin Rivers. ECHAM3 roughly simulates the U.S.-wide pattern: most of the northern (southern) parts of the country experience a decrease (increase) in the frequency of heavy precipitation. Significantly strong frequency decreases and increases occur in the northern Rockies and along the Gulf Coast, respectively, both in excellent agreement with observations. In disagreement with observations, California experiences a significant modeled increase in the frequency of heavy rainfall during warm winters with a maximum in southern California amounting to a twofold to threefold increase from base years.

Lower panels of Fig. 2 show the La Niña signal in heavy rainfall frequency. This is manifested in nature in a general reversal of the El Niño pattern with increased (decreased) frequencies in much of the northern (southern) United States. The significant part of this pattern is limited to more frequent heavy rainfall to the south of the Great Lakes (Ohio–Mississippi River valley) and a strong decrease of 30%–50% in and immediately around northern Florida. The model shows some agreement with observations in the southeast but overestimates (by ~30%) the decrease of heavy rainfall frequency in Texas. The strongest model La Niña signal is in full disagreement with observations: an intense (twofold to threefold) *increase* in the southwest stretching and diminishing into the western Rockies.

In the western United States, general agreement exists between ENSO patterns observed here and those previously documented by other workers (e.g., Cayan et al. 1996; Woolhiser et al. 1993). However, in our analysis, these patterns are mostly not statistically significant. It is possible that statistical significance is diminished by treating the warm and cold ENSO phases separately, as opposed to describing the ENSO signal as it is commonly described in the literature: either as the difference between the warm and cold phase composites, or in the form of correlations with the Southern Oscillation index. We have treated the warm and cold ENSO phases separately, because there is no basis for assuming that the ENSO teleconnections are generally linear. In fact, evidence to the contrary is presented throughout this paper. While this paper was in review, it came to our attention that physical reasons for nonlinearity of ENSO teleconnections have been recently explored by Hoerling et al. (1997).

The heavy rainfall anomaly patterns described above are qualitatively similar to comparable patterns of total anomalous winter rainfall amount (not shown), reflecting the important contribution of heavy rainfall to total seasonal precipitation.

b. Temperature extremes

In base years, 90% of the winter days are marked with average temperature between the 95th and 5th percentiles. The temperatures associated with these percentiles are displayed in the upper panels of Figs. 3 and 4, respectively. As was the case with precipitation quantiles, spatial patterns of observed and modeled base years' 95th and 5th DJF daily temperature percentile are in close general agreement. The effect of the Rockies is more spatially extensive in the model climate due to the coarse spatial resolution. However, in both model and observations, the Rockies are better delineated on *warm* extreme (95th percentile) maps since high elevations exert a rigid *upper* limit on ambient temperatures. Model and observations also agree that the southwestern coast is characterized by colder warm extremes compared to the southeastern and gulf coasts. This is due to the cool influence of the California Current. There are noteworthy disagreements between model and observations, however. The model underestimates the 95th percentile over the western United States by about 5°C, producing warm extremes that are not quite warm enough. In the central (all latitudes) and southeastern United States, ECHAM3 overestimates the 5th percentile by as much as 7°C, suggesting that modeled cold outliers are not as cold as those in nature.

ENSO signals in the frequency of extreme warm days (temperatures above the 95th base percentile) are presented in Fig. 3, middle and lower panels for El Niño and La Niña winters, respectively, and ENSO signals in the frequency of extreme cold days (temperatures below the 5th base percentile) are presented in Fig. 4. As before, nature is on the left, while ECHAM3 is on the right. In the following discussion, nature is referred to unless otherwise stated.

The El Niño pattern in the U.S. DJF warm temperature extremes is a frequency increase by 20%–40% in the Midwest and a frequency decrease throughout most of the rest of the country. The signal, however, is limited to the southern United States: New Mexico and Texas (>60% decrease) and the deep south (>40% decrease) except for Florida and Georgia. ECHAM3 misses the general structure of the observed pattern by increasing (decreasing) frequencies of warm extremes in the west (east), in effect rotating the observed pattern counterclockwise by 90°.

It is interesting to note that the observed large-scale El Niño patterns in warm and cold temperature extremes add up to an almost U.S.-wide decrease in wintertime intraseasonal temperature variability (both tails tend to contract). However, because this pattern is not highly significant, we merely note but do not pursue this possibility any further.

The La Niña pattern in warm extremes is *not* the exact inverse of the El Niño pattern. During La Niña winters, the northwestern part of the country and the West Coast experience reduced frequencies of warm extremes (most notably northeastern Montana and Washington, by over 40%), while the eastern-southeastern portion of the United States enjoys more warm extremes (by more than 50% of base years' frequencies in much of the region).

The modeled pattern is surprisingly similar to the one observed, although the enhancement of warm extreme frequencies is overestimated. The geographical center of this enhancement is in Texas, rather than farther to the east, as in observations. The magnitude of the enhancement there is over 240% of model base frequencies. Even in the southeast, warm extreme frequencies are enhanced by over 140% relative to modeled base values, a value far greater than that observed. The reduction in frequency of warm outbreaks in the northwest is comparable with observations but more of it is statistically significant.

The following ENSO patterns are evident in the frequencies of cold outbreaks. During El Niño winters, most of the contiguous United States shows a reduction in the frequency of cold outbreaks. Most of the largest reductions (e.g., >40% east of the Cascades) are not statistically significant; however, signal is observed in eastern Colorado, in the vicinity of the Great Lakes, and in Maine. As with the El Niño signal in warm outbreak frequencies, ECHAM3 does not capture the structure of the above large-scale pattern in cold outbreak frequencies. The modeled El Niño signal is patchy and characterized by increased frequencies of cold outbreaks around the Gulf Coast and Virginia.

During La Niña years, the patterns for cold extreme frequency anomalies are roughly inverses of those for warm extremes with more cold outbreaks in the northwestern/western part of the country and fewer cold outbreaks in the east excluding New England (Fig. 4, lower-left panel). The signal, however, is limited to decreased frequency of cold outbreaks around Virginia and increased frequency in southern California.

The model produces a decrease in cold outbreaks in the south-central United States, along the Gulf Coast, but the rest of the United States undergoes an increase in the frequency of extreme cold events that is much too strong (over 100% increase in many regions) even in the areas of sign agreement with observations. For cold outbreaks, the model is not as geographically accurate as for warm outbreaks associated with La Niña. A common shortcoming of the model response to La Niña is the overestimation of both warm and cold event frequency anomalies in regions of positive modeled anomalies. In other words, for those locations where the model produces an increase in extreme temperature frequencies associated with the cold ENSO phase, it tends to overinflate the tails of the wintertime daily temperature PDF.

c. Temperature central tendency

To shed more light on how the entire distribution of wintertime intraseasonal temperature adjusts to ENSO forcing, we describe the changes in central tendency that accompany the changes in the frequency of extremes described above. For consistency of interpretation, we depict central tendency in terms of frequency of above-median (50th percentile) daily temperature. As with extreme quantiles, median wintertime daily temperature is defined for base years and has a spatial distribution (not shown) similar to that of the 95th temperature percentile for both observations and model (upper panels of Fig. 3). The ENSO signal in temperature central tendency is then described as the frequency anomaly of above-median base winters' daily temperature. The spatial distributions of above-median temperature frequency anomalies due to El Niño and La Niña forcing are presented in Fig. 5, top and bottom plates, respectively. As before, model results are on the right and nature is on the left. In light of the extreme event frequency anomalies presented in the previous subsection, and focusing on large-scale signals, the central tendency results can be summarized as follows.

During El Niño, the northern (southern) part of the country experiences a positive (negative) shift in temperature central tendency, agreeing with the common understanding of the El Niño signal in winter mean temperature anomalies (e.g., Ropelewski and Halpert 1986). In terms of temperature central tendency, the middle zone of the country remains largely unaffected by El Niño. *In general, significant shifts in the temperature central tendency do not necessarily translate into significant shifts in the tails, whereas signals in the tails are not necessarily manifestations of shifts in the central tendency.* The Midwestern shift in central tendency, for example, is not reflected in extreme temperature frequency signals. The decreased frequency of cold extremes in Maine (Fig. 4, middle left panel) occurs without a significant shift in central tendency. Even U.S.-wide El Niño patterns in extreme frequencies do not follow that in the central tendency. The extreme warm (cold) temperature frequency El Niño pattern resembles the central tendency pattern, but shifted about 5°–10° to the north (south).

Modeled temperature central tendency anomalies are stronger than those observed. The modeled above-median frequency El Niño anomaly pattern is similar to the modeled extreme patterns. This implies that the model responds to El Niño forcing by shifting its temperature PDFs, thereby inflating the forward tail (i.e., the tail toward which the PDF shift occurs).

The La Niña winter observed above-median frequency anomaly pattern (Fig. 5, bottom-left panel), is in general spatial agreement with the warm and cold extreme frequency anomalies (bottom-left panels of Figs. 3 and 4, respectively). This suggests that, during the cold ENSO phase, shifts in the PDFs commonly occur together with extensions (contractions) of the forward (rear) tail. However, except for southern California, statistically significant signals in the central tendency do not generally translate into statistically significant signals in the tails and visa versa, suggesting that ENSO can act semi-independently on various quantile ranges of the daily local U.S. wintertime temperature distributions.

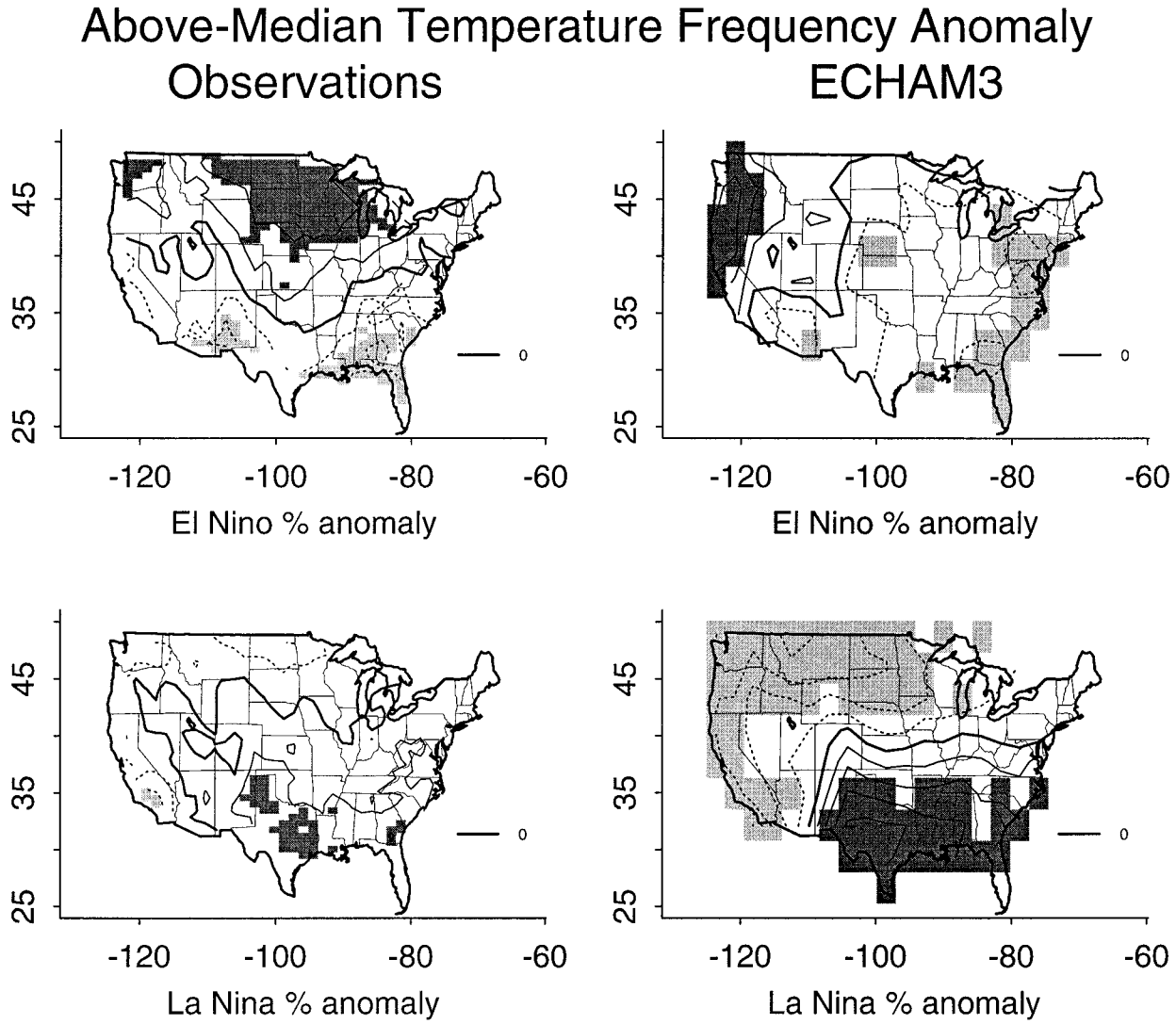

FIG. 5. (upper panels) Percentage anomaly of observations during warm years *warmer* than the base years' 50th percentile (i.e., median). The zero contour is thickened. Negative (positive) contours are dashed (solid), delineated at 10% intervals. Positive (negative) values found to be statistically significant at the 0.1 significance level are darkly (lightly) shaded. (lower panels) Same as upper panels but for cold years. (left panels) Observational results. (right panels) Model results.

Corresponding modeled patterns are consistent with the interpretation that, as during El Niño, modeled temperatures respond to the cold phase of ENSO with shifts in the PDFs and inflation of the forward tail. One area of exception is the eastern midsection of the country (35°–40°N, east of 100°W), where both tails are inflated (i.e., variance increases) without an accompanying shift in central tendency.

5. Summary and conclusions

Consistent signals exist in the wintertime frequency of heavy rainfall and extreme temperature events associated with the opposite phases of ENSO. Their salient features are summarized below. Except for the modeled La Niña signals, temperature and precipitation extreme anomalies tend to be locally decoupled from each other in both model and observations.

Increased (decreased) frequencies of heavy rainfall, defined here as daily rainfall exceeding the base winters' 75th percentile, are observed during warm (cold) years in the southern portion of the country and much of the Great Plains. The northern portion of the country exhibits patterns of opposite phase. These patterns are statistically significant in the Southeast, Gulf Coast, northern Rockies, and the general area of the Mississippi–Ohio River valleys. Long-range statistical prediction of the wintertime frequency of heavy rainfall events seems possible in these areas of the contiguous United States (to be explored in a future paper). Although we do find ENSO patterns in heavy rainfall frequency in the western United States consistent with those found by others

(e.g., Cayan et al. 1996; Woolhiser et al. 1993), in our analysis these patterns are, for the most part, not statistically significant at the 0.1 significance level.

Given known difficulties associated with GCM representation of the hydrologic cycle (e.g., IPCC 1990), ECHAM3 does a remarkably good job (after correcting model tendency to produce drizzle) of modeling the spatial distribution of the upper wintertime rainfall quantiles in base years. However, the GCM results are somewhat contradictory, since ECHAM3 captures the approximate spatial features of the ENSO signal in heavy rainfall frequency but errs in estimating signal amplitude. This flaw can presumably be statistically corrected for predictive purposes. In detail, the model also shows major regional discrepancies with observations in the sign of the signal. The most glaring example of this is the profound enhancement of heavy rainfall frequencies in the southwest during cold phases of the ENSO cycle. Such regional errors may be due the apparent lack of interannual variability in modeled *global* atmospheric moisture content (L. Goddard 1996, personal communication). In any event, the GCM is not capturing the small spatial-scale details of the ENSO signal.

On continental scales, however, ECHAM3 results suggest that the GCM hydrologic cycle can be sensitive (usually in the correct sense) on intraseasonal timescales to low-frequency forcings. This conclusion lends some support to the idea that GCMs are capable of predicting large-scale changes in extreme rainfall frequencies due to low-frequency climatic forcing such as doubling of CO_2. However, attempts at regional interpretations of such predictions are misguided, as we noted above. More germane to the goals of this work, our conclusions provide restrained encouragement to attempts at using GCMs for long-range prediction of intraseasonal hydrologic variability, although multiple model realizations would be required for skillful prediction (see below).

The large-scale ENSO patterns and regional signals differ substantially in different quantile ranges of the U.S. wintertime daily temperature PDFs. This suggests that ENSO can force shifts in the central tendency of intraseasonal PDFs as well as change their shapes. Significant central tendency shifts toward warmer temperature observed in the Midwest during El Niño winters, for example, do not translate into significant extreme temperature frequency anomalies. On the other hand, signals in warm and cold extreme temperature frequencies in the eastern United States during La Niña winters are accompanied by only an insignificant shift in central tendency. The U.S.-wide El Niño patterns in extreme warm and cold temperature frequencies resemble the observed central tendency pattern shifted 5°–10° north and south, respectively. During La Niña winters, however, U.S.-wide patterns in extreme temperature frequencies tend to be more spatially consistent with the central tendency pattern. Moreover, it appears that the warm tail of the wintertime intraseasonal temperature PDFs is generally more sensitive to both ENSO extremes than the cold tail. Elucidation of the physical processes producing these signals would require regionally focused studies including examination of atmospheric circulation patterns and separate analyses of daily maximum and minimum temperatures.

In the modeled climate, ENSO manifests itself primarily through wholesale shifts in the daily temperature PDFs. As in the observations, these are somewhat less consistent in various PDF quantile ranges during warm winters and more consistent during cold winters. It must be noted, however, that the large-scale El Niño patterns have almost no resemblance to those observed. The model temperature response to El Niño is likely caused by an incorrect modeling of the atmospheric teleconnection pattern. This warrants a more detailed investigation. Large-scale La Niña patterns, on the contrary, are in much better agreement with the observations. However, extreme temperature frequency anomalies are severely exaggerated. Apparently, modeled shifts in central tendency translate into overinflation of the forward tail during La Niña winters. The model's preference for this kind of behavior during the cold phase of ENSO, when the general agreement with observations is better than during the warm phase, is rather puzzling. Because observed extreme temperature frequency anomalies do not appear to be strictly related to shifts in central tendency, model output cannot be simply statistically corrected if the model is to be used for prediction of intraseasonal extreme frequencies.

There are many puzzling ways in which nonlinearity of ENSO teleconnections manifests itself regionally in U.S. wintertime intraseasonal statistics. Some observed examples are as follows.

- The central Rockies tend to receive more frequent heavy precipitation during El Niño winters. No other ENSO signals are observed there in any of the other frequency variables considered.
- In the Ohio/Mississippi valley, more frequent heavy precipitation events during La Niña winters are accompanied by more frequent extreme warm temperature events associated with a general shift of the temperature PDF toward warmer conditions. During El Niño winters, no signal is observed in any of the frequency variables.
- The Gulf Coast experiences more frequent heavy rainfall events accompanied by *cooler* temperatures and less frequent extreme warm temperature events during El Niño winters. During La Niña winters, the decrease in heavy rainfall frequency is confined to the eastern Gulf Coast without a correspondingly coherent temperature signal there.
- While large-scale El Niño and La Niña patterns in temperature central tendency tend to be roughly inverses of each other, large-scale patterns in comparable extreme temperature frequencies differ. These

differences likely stem from differences in how the warm and cold phases of ENSO affect the entire regional intraseasonal temperature PDFs.
- Warm tails of the wintertime daily temperature PDFs are more sensitive to ENSO forcing than cold tails.

These are examples of the nonlinearity of ENSO teleconnections within and between regions. Moreover, the term ''regions'' is not limited to its geographical meaning, but also applies to PDF quantile regions. It is clear that GCM physics do not reproduce these observed regional signals, although the signals they produce are also nonlinear. An effort to explain the observed and modeled behavior region by region would be a challenging and useful undertaking.

The canonical signature of ENSO in the U.S. surface winter climate can be approximated to varying degrees of precision with a multidecadal run of a state-of-the-art atmospheric GCM forced with global SST. However, as we expected, and found, the GCM had no skill (results not shown) in predicting individual winter's intraseasonal statistics. The need for an ensemble forecast approach to the estimation of intraseasonal variability is clear (cf., e.g., Barnett 1995; Lau et al 1996). Such ensemble GCM climate prediction attempts could be justified on continental scales for parts of the world where well-resolved and sufficiently long observational data are not available. However, in those parts of the world where long quality daily records are available, a simpler, perhaps more skillful approach to the long-range intraseasonal climate prediction problem is through the use of conditional PDFs derived from past empirical records. Work toward this goal is in progress. For now, we simply note that knowledge about the roles that severity of ENSO phases and decadal modes of climate variability play in modulating the signals described here would also be of great value to regional statistical long-range climate prediction.

Acknowledgments. Support for this work was provided through the UC Campus Laboratory Collaboration Program and NSF Grant ATM-93-14495. Thanks are due to T. Karl of NCDC for the observational data and L. Bengtsson of MPI for the ECHAM3 model. D. Cayan contributed intellectually through many thought-provoking discussions. Comments by two anonymous reviewers significantly improved the quality of the manuscript.

REFERENCES

Barnett, T. P., 1995: Monte Carlo climate forecasting. *J. Climate,* **8,** 1005–1022.

——, N. Graham, M. Latif, S. Pazan, and W. White, 1993: ENSO and ENSO-related predictability. Part I: Prediction of equatorial Pacific sea surface temperature with a hybrid coupled ocean–atmosphere model. *J. Climate,* **6,** 1545–1566.

Barrow, E. M., and M. Hulme, 1996: Changing probabilities of daily temperature extremes in the UK related to future global warming and changes in climate variability. *Climate Res.,* **6,** 21–31.

Brown, B. G., R. W. Katz, and A. H. Murphy, 1986: On the economic value of seasonal precipitation forecasts: The fallowing/planting problem. *Bull. Amer. Meteor. Soc.,* **67,** 883–841.

Cane, M. A., and S. E. Zebiak, 1985: A theory for El Niño and the Southern Oscillation. *Science,* **228,** 1085–1087.

Cayan, D. R., and R. H. Webb, 1992: El Niño/Southern Oscillation and streamflow in the western United States. *El Niño: Historical and Paleoclimatic Aspects of the Southern Oscillation,* H. F. Diaz and V. Markgraf, Eds., Cambridge University Press, 29–88.

——, K. Redmond, and L. Riddle, 1996: Accentuated ENSO effects on extreme hydrologic events over the western United States. Preprints, *21st Annual Climate Diagnostics and Prediction Workshop,* Huntsville, AL, Climate Prediction Center, 324–325.

Changnon, S. A., and D. Vonnahme, 1986: Use of climate predictions to decide a water management problem. *Water Resour. Bull.,* **22,** 649–652.

Chen, M., R. E. Dickinson, X. Zeng, and A. N. Hahmann, 1996: Comparison of precipitation observed over the continental United States to that simulated by a climate model. *J. Climate,* **9,** 2233–2249.

Cubasch, U., J. Waszkewitz, G. Hegeri, and J. Perlwitz, 1995: Regional climate changes as simulated in time-slice experiments. *Climate Change,* **31,** 273–304.

Efron, B., 1982: *The Jackknife, the Bootstrap, and Other Resampling Plans.* Society for Industrial and Applied Mathematics, 92 pp.

Graham, N. E., and T. P. Barnett, 1995: ENSO and ENSO-related predictability. Part II: Northern Hemisphere 700-mb height predictions based on a hybrid coupled ENSO model. *J. Climate,* **8,** 544–549.

——, ——, M. Ponater, and S. Schubert, 1994: On the roles of tropical and midlatitude SSTs in forcing interannual to interdecadal variability in the winter Northern Hemisphere circulation. *J. Climate,* **7,** 1416–1441.

Gregory, J. M., and J. F. B. Mitchell, 1995: Simulation of daily variability of surface temperature and precipitation over Europe in the current and $2 \times CO_2$ climates using the UKMO climate model. *Quart. J. Roy. Meteor. Soc.,* **121,** 1451–1476.

Hoerling, M. P., A. Kumar, and M. Zhong, 1997: El Niño, La Niña, and the nonlinearity of their teleconnections. *J. Climate,* **10,** 1769–1786.

Intergovernmental Panel on Climate Change, 1990: *The IPCC Scientific Assessment.* J. T. Houghton, G. J. Jenkins, and J. J. Ephraums, Eds., Cambridge University Press, 364 pp.

Kiladis, G. N., and H. Diaz, 1989: Global climatic anomalies associated with extremes in the Southern Oscillation. *J. Climate,* **2,** 1069–1090.

Lau, K.-M., J. H. Kim, and Y. Sud, 1996: Intercomparison of hydrologic processes in AMIP GCMs. *Bull. Amer. Meteor. Soc.,* **77,** 2209–2227.

Lau, N. G., 1985: Modeling the seasonal dependence of the atmospheric response to observed El Niños in 1962–76. *Mon. Wea. Rev.,* **113,** 1970–1996.

Pan, W. H., L. A. Li, and M. J. Tsai, 1995: Temperature extremes and mortality from coronary heart disease and cerebral infarction in elderly Chinese. *Lancet,* **345,** 353–355.

Redmond, K. T., and D. R. Cayan, 1994: El Niño/Southern Oscillation and western climate variability. Preprints, *Sixth Conf. on Climate Variations,* Nashville, TN, Amer. Meteor. Soc., 141–145.

Ropelewski, C. F., and M. S. Halpert, 1986: North American precipitation and temperature patterns associated with the El Niño/Southern Oscillation (ENSO). *Mon. Wea. Rev.,* **114,** 2352–2362.

——, and ——, 1996: Quantifying Southern Oscillation—Precipitation relationships. *J. Climate,* **9,** 1043–1059.

Wallace, J. M., and D. S. Gutzler, 1981: Teleconnections in the geopotential height field during the Northern Hemisphere winter. *Mon. Wea. Rev.,* **109,** 784–812.

Woolhiser, D. A., T. O. Keefer, and K. Redmond, 1993: Southern Oscillation effects on daily precipitation in the southwestern United States. *Water Resour. Res.,* **29,** 1287–1295.